ELSEVIER

Journal of Molecular Catalysis B: Enzymatic 6 (1999) 533–547

JOURNAL OF MOLECULAR CATALYSIS B: ENZYMATIC

Kinetic characterization of chiral biocatalysis of cycloarenes by the camphor 5-monooxygenase enzyme system [1]

David A. Grayson [a,*], Vincent L. Vilker [b]

[a] *Department of Chemical Engineering, University of California at Los Angeles, Los Angeles, CA 90095, USA*
[b] *Biotechnology Division, National Institute of Standards and Technology, Gaithersburg, MD 20899, USA*

Received 2 July 1998; accepted 14 October 1998

Abstract

Redox enzyme mediated biocatalysis has the potential to regio- and stereo-specifically oxidize hydrocarbons producing valuable products with minimal by-product formation. In vitro reactions of the camphor (cytochrome *P*-450) 5-monooxygenase enzyme system with naphthalene-like substrates yield stereospecifically hydroxylated products from nonactivated hydrocarbons. Specifically, the enzyme system catalyzes the essentially stereospecific conversion of the cycloarene, tetralin (1,2,3,4-tetrahydronaphthalene) to (*R*)-1-tetralol ((*R*)-(−)-1,2,3,4-tetrahydro-1-naphthol). It is shown that this reaction obeys Michaelis–Menten kinetics and that interactions between the enzyme subunits are not affected by the identity of the substrate. This subunit independence extends to the efficiency of NADH usage by the enzyme system—subunit ratios do not effect efficiency, but substrate identity does. Tetralin is converted at an efficiency of $13 \pm 3\%$, whereas (*R*)-1-tetralol is converted at $7.8 \pm 0.7\%$. A model of this system based on Michaelis–Menten parameters for one subunit (Pdx: $K_M = 10.2 \pm 2$ μM) and both substrates (tetralin: $K_M = 66 \pm 26$ μM, $\nu_{max} = 0.11 \pm 0.04$ s^{-1}, and (*R*)-1-tetralol: $K_M = 2800 \pm 1300$ μM, $\nu_{max} = 0.83 \pm 0.22$ s^{-1}) is presented and used to predict the consumption and production of all substrates, products and cofactors. Published by Elsevier Science B.V.

Keywords: Biocatalysis; Camphor 5-monooxygenase; Cytochrome $P\text{-}450_{cam}$ hydroxylase; Decalin; Michaelis–Menten kinetics; Naphthalene; Stereochemistry; Stoichiometry; Tetralin

1. Introduction

Regioselective hydroxylation of aromatic and alicyclic hydrocarbons can lead to valuable intermediates useful to the agrochemical, pharmaceutical, petrochemical, and flavor industries. The cytochrome *P*-450 monooxygenases, of which there are now more than 300 known forms, representing a wide range of substrate specificities, catalyze the regio- and stereospecific hydroxylation of compounds starting from substrates that have few or no functional groups. These biocatalysts are found in many types of microbial, plant, insect and mammalian cells and have great potential for carrying out value-added biotransformations and contaminant biodegradation. The effective utilization of these biocatalysts requires data on the nature of potential substrates and cofactors, and on the thermodynamics and kinetics of the reactions catalyzed. Also, any mechanistic picture of the

* Corresponding author. Present address: 3061 Maplewood Place, Escondido, CA 92027, USA.

[1] Use of trade names is for identification only and does not constitute endorsement by the National Institute of Standards and Technology.

1381-1177/99/$ - see front matter Published by Elsevier Science B.V.
PII: S1381-1177(99)00003-X

reaction must be consistent with such phenomenological results.

The enzyme system camphor (cytochrome *P*-450) 5-monooxygenase (EC 1.14.15.1) consists of three protein subunits: putidaredoxin reductase (PdR), relative molecular mass $M_r = 43{,}500$; putidaredoxin (Pdx), $M_r = 11{,}600$; and cytochrome $P\text{-}450_{cam}$ hydroxylase (Cyt-m), $M_r = 45{,}000$. NADH is used as a reducing source. In vitro, this system has been shown to exhibit wide-ranging biotransformation capabilities including hydroxylation of camphor-like structures [1,2], regiospecific oxidation of benzene derivatives [3,4], and oxidative and reductive dehalogenation of aliphatic halocarbons [5–7]. Rationalization of substrate selectivity and product distribution has often been based on the structure [8] of the catalytic site, i.e., the heme pocket located in the hydroxylase protein.

Previously, Grayson et al. [9] established that camphor 5-monooxygenase mediated biohydroxylation of tetralin to (*R*)-1-tetralol:

$$\text{tetralin(aq)} + \text{NADH}^{-2}\text{(aq)} + \text{O}_2\text{(aq)} + \text{H}^+\text{(aq)} \rightleftarrows (R)\text{-1-tetralol(aq)} + \text{NAD}^-\text{(aq)} + \text{H}_2\text{O}(l) \quad \text{(A1)}$$

is essentially an 'irreversible' reaction, $K_{eq} \approx 4 \times 10^{65}$. The driving force of this reaction, the large enthalpy of formation of water and the large difference between the enthalpy of formation of substrate (tetralin(l)) and hydroxylated product ((*R*)-1-tetralol(s)), is common to all camphor 5-monooxygenase mediated hydrocarbon biohydroxylations. This suggests that biohydroxylation is thermodynamically very favorable for hydrocarbon substrates. In fact, Peterson et al. [10] obtained similar favorable thermodynamics for the biohydroxylation of camphor to (+)-5-*exo*-hydroxycamphor. This paper presents the results obtained from investigating the biocatalytic ability of camphor 5-monooxygenase to hydroxylate unnatural substrates.

We report herein that camphor (cytochrome *P*-450) 5-monooxygenase, originally isolated from the bacterium *Pseudomonas putida* PpG 786, hydroxylates non camphor-like hydrocarbon substrates; naphthalene, 1,2,3,4-tetrahydronaphthalene (tetralin) and decahydronaphthalene (decalin). DMSO can be used as an accelerator for biohydroxylation of hydrocarbon substrates, but at high concentrations, it inhibits the reaction. It was also found that the Michaelis–Menten dissociation constant for the Pdx–Cyt-m complex was not effected by substrate identity. NADH efficiency, expressed as the stoichiometric relationship between NADH usage and substrate disappearance, is independent of Pdx concentration, but strongly dependent upon the identity of the substrate. Kinetic studies were undertaken to determine the effect of unnatural substrates on catalytic ability, resulting in a Michaelis–Menten based model of the stereospecific bioconversion of tetralin to (*R*)-1-tetralol.

2. Experimental

2.1. Chemicals and buffers

The principal substances used in this study, their respective Chemical Abstracts Services (CAS) registry numbers, empirical formulas, molecular weights and suppliers are: 1,2,3,4-tetrahydronaphthalene (tetralin), 119-64-2, $C_{10}H_{12}$, 132.205, Aldrich; 1,2,3,4-tetrahydro-1-naphthol (1-tetralol), 529-33-9, $C_{10}H_{12}O$, 148.205, Aldrich; (*R*)-(−)-1,2,3,4-tetrahydro-1-naphthol ((*R*)-1-tetralol), 23357-45-1, $C_{10}H_{12}O$, 148.205, Sigma; (*S*)-(+)-1,2,3,4-tetrahydro-1-naphthol ((*S*)-1-tetralol), 53732-47-1, $C_{10}H_{12}O$, 148.205, Sigma; decahydronaphthalene mixture of *cis* 493-01-6 and *trans* 493-02-7, $C_{10}H_{18}$, 138.25, Aldrich; (±)-norcamphor (2-norbornanone), 22270-13-9, $C_7H_{10}O$, 110.16, Sigma; naphthalene, 91-20-3, $C_{10}H_8$, 128.17, Aldrich; (1*R*)-(+)-camphor, 464-49-3, $C_{10}H_{16}O$, 152.24, Sigma; β-nicotinamide adenine dinucleotide (NAD), 53-84-9, $C_{21}H_{27}N_7O_{14}P_2$, 663.431, Sigma; and β-nicotinamide adenine dinucleotide, reduced form, disodium salt (NADH), 606-68-8,

$C_{21}H_{27}N_7O_{14}P_2Na_2$, 709.411, Sigma. Lysozyme chloride, ampicillin, cytochrome c, and deoxyribonuclease I were from Sigma. The other substances used in this study were reagent grade chemicals purchased from Fisher Scientific, Pittsburgh, PA. Purified water for all media and experiments was obtained from a Millipore, Milli-q system with an HPLC-grade organic scavenging cartridge.

The following buffers were used: P-0, 0.02 M KH_2PO_4, adjusted to pH 7.4 with $\approx$2 M KOH; P-100, 0.02 M KH_2PO_4, 0.1 M KCl, adjusted to pH 7.4 with $\approx$2 M KOH; T, 20 mM Tris–HCl, pH adjusted to 7.4 with $\approx$1 M Tris base.

2.2. Preparation of enzyme system

2.2.1. Growth and purification

DH5-α *Escherichia coli* clones of the three enzyme subunits: putidaredoxin (Pdx), putidaredoxin reductase (PdR) and cytochrome *P*-450_{cam} hydroxylase (Cyt-m), were provided by Professor Julian A. Peterson of the University of Texas Southwestern Medical Center, Dallas, TX. Using previously reported methods [7,9], separate growth and purification of each subunit eliminated the threat of cross-contamination and provided much higher yields of the purified proteins than those obtained from the natural host, *P. putida*. Information on the yield, purity and activity [7,11] for each protein subunit is summarized in Table 1. As previously reported [9], the spectroscopically measured purity of the subunits was over 90% and using high-resolution two-dimensional gel electrophoresis as described by Edwards et al. [12] mole fraction purity was estimated to be greater than 97%.

2.3. Analytical

2.3.1. Gas chromatography

A Varian 3700 GC equipped with a flame ionization detector and a J&W Scientific DB-5 Megabore column (length = 30 m, i.d. = 0.53 mm) coated with a phenyl-substituted methylpolysiloxane phase (mass fraction = 0.05, film thickness = 1.5×10^{-6} m) was used for quantification of tetralin, 1-tetralol, decalin, naphthalene and norcamphor. The temperatures of the injector port and detector were, respectively, 250°C and 300°C. Helium was used as the carrier gas; its head pressure was $\approx$4.1 bar. The volume of sample injected was 2 μl. For tetralin and 1-tetralol detection, the following temperature gradient was used for the column oven: 80°C at $t = 0$; at $t = 17$ min, the temperature was increased at a rate of 4 K min^{-1} until a final temperature of 295°C was reached; this temperature was maintained for 8 min. The respective retention times for tetralin and 1-tetralol were 24 min and 33 min. Decalin, naphthalene and norcamphor were detected using the following temperature gradient for the column oven: 70°C at $t = 0$; at $t = 6$ min, the temperature was increased at a rate of 10 K min^{-1} until a final temperature of 295°C was reached; this temperature was maintained for 8 min. The

Table 1
Characterization of protein purification

Protein	Yield $\times 10^3$ [a]	$A(\lambda_1)/A(\lambda_2)$ [b]	Activity [c] (nmol mg^{-1} s^{-1})
putidaredoxin reductase (PdR)	1.1 to 1.3	0.13 to 0.14	220 to 250
putidaredoxin (Pdx)	2.5 to 3.6	0.44 to 0.48	410 to 580
cytochrome *P*-450_{cam} hydroxylase (Cyt-m)	1.8 to 2.5	1.5 to 1.6	230 to 380

[a] Yield is defined as (mass of protein/mass of wet cell paste).
[b] The absorbance ratio $A(\lambda_1)/A(\lambda_2)$ was determined for the following wavelengths λ: $\lambda_1 = 454$ and $\lambda_2 = 275$ nm for PdR; $\lambda_1 = 455$ and $\lambda_2 = 275$ nm for Pdx; and $\lambda_1 = 392$ and $\lambda_2 = 280$ nm for Cyt-m.
[c] The activity of PdR and Pdx is (amount of cytochrome c reduced)/(mass of protein $\times$ time) as determined by the method described by Phillips and Langdon [11]. The activity of Cyt-m is (amount of (1*R*)-(+)-camphor hydroxylated)/(mass of protein $\times$ time) as determined by the method described by Koe and Vilker [7].

respective retention times for norcamphor, *trans*-decalin, *cis*-decalin and naphthalene were 9.2, 11.0, 11.9 and 13.4 min.

2.3.2. High performance liquid chromatography

HPLC was used for the quantification of tetralin, (*R*)-1-tetralol, (*S*)-1-tetralol, 1-tetralone and 2-tetralone. The system used was a Beckman System Gold Programmable Detector Module 166 equipped with a Beckman 110B solvent-delivery module, a Beckman 427 integrator, a NEC PC-8300 and a Chiralcel OB-H column (length = 15 cm, i.d. = 0.46 cm) kept at room temperature. The mobile phase was (95 vol.% hexane + 5 vol.% isopropyl alcohol); the flow rate was 0.5 ml min^{-1}. The sample was introduced to the column using a calibrated injection loop (volume = 100 μl) and the wavelength of the detector was set at 254 nm. Under these conditions, the respective retention times for tetralin, (*R*)-1-tetralol, (*S*)-1-tetralol, 1-tetralone and 2-tetralone were 4.9, 9.5, 14, 16.5 and 22 min.

2.3.3. Gas chromatography-mass spectrometry

Methylene chloride extracts were prepared for GC-MS analysis in a manner identical to the hexane extract preparation (see Section 2.4.2). Concentrates from the methylene chloride phase of the extracted sample were used as 1.5 μl splitless injections onto the GC-MS. The GC-MS measurements were performed with a Finnigan 9610 GC (Finnigan/MAT, Sunnyvale, CA) equipped with a J&W Scientific DB-5 capillary column (length = 30 m, i.d. = 0.25 mm) interfaced with a Finnigan 4000 mass spectrometer (electron energy = 70 eV, ion source temperature = 270°C, ion source pressure = 1.0×10^{-4} Pa and emission current = 0.5 mA). The injector and detector temperatures were 280°C. The column temperature was held at 30°C for 4 min and then increased at a rate of 6 K min^{-1} to a final temperature of 300°C. The spectral data were recorded using an Incos data system at a scan rate of 1 s $decade^{-1}$. Spectral data were matched with those in the EPA-NIH Spectral Database [13].

2.3.4. Spectrophotometry

Although HPLC, GC and GC-MS were able to measure most of the species involved in the hydroxylation reactions, NADH was tracked using a Beckman DU®-65 Spectrophotometer. The spectrophotometer was blanked either with a buffer solution or with a control solution as appropriate for the experiment. Samples were placed in 1.5 ml cuvettes and the absorbance at 340 nm was recorded. This absorbance was converted into NADH concentration using the extinction coefficient 6.22 mM^{-1} cm^{-1}. Samples with $A_{340\ nm}$ over 1, corresponding to solutions with over ≈160 μM NADH, were diluted with known quantities of P-100 in order to bring measurements back into the linear range of the instrument.

2.4. Hydroxylation reactions

2.4.1. Pre-reaction subunit cleaning

Purified enzyme solutions were prepared for reactions in a two-column procedure. After thawing in an ice bath, the three purified subunits were separately concentrated using Millipore Ultrafree-CL centrifugal filter units with a 10,000 nominal molecular mass cutoff. Camphor was removed from the purified Cyt-m by a method adapted from Gunsalus and Wagner [14]. Cyt-m solutions were made 50 mM in DTT and incubated for 15 to 20 min at 22°C. Camphor and DTT were removed by gel filtration on a Sephadex G-10 column (Pharmacia, length = 20 cm, i.d. = 1 cm), equilibrated with the buffer T. The effluent Cyt-m was concentrated with the above-mentioned filter unit. Then, thawed Pdx and PdR and the reconcentrated Cyt-m were individually passed through a second Sephadex G-10 column (Pharmacia, length = 40 cm, i.d. = 1 cm) with the reaction buffer P-100. This chromatographic step was necessary to serve as a buffer exchange and to remove any remaining camphor or DTT from

the proteins. All preparations of enzyme solutions, unless noted otherwise, were carried out at 4°C. If the enzyme preparations were not used within 1 h, the solutions were stored in an argon environment.

2.4.2. Hydroxylation reaction mixtures

Hydroxylation reactions were performed to determine product identification, substrate–NADH stoichiometry and kinetic parameters. The prepared enzyme subunits were first mixed with P-100 and DMSO dissolved substrate in a Teflon flask to make a master solution. The master solution consisted of 118 μM substrate, 0.44% vol/vol DMSO, 3.55 μM Cyt-m, 3.55 μM PdR, 35.5 μM Pdx and 80–99% vol/vol P-100. Teflon vessels were used in place of glass vessels to minimize the chance of adsorption of tetralin on the walls of the master flask. A volume of 2.75 ml of the master solution was pipetted into each of the 5 ml glass reaction vials and sealed with a Teflon coated rubber septum. The Teflon coating eliminated the possibility of dissolution of the rubber into the solution. Reactions were started by the addition to each reaction vial of 0.5 ml of 24 mM NADH dissolved in P-100. P-100 without NADH was added to start non-reacting control vials. The vials were then shaken at ≈100 rpm at room temperature. The initial reacting contents of a typical reaction vial were 80–99% vol/vol P-100, 0.37% vol/vol DMSO, 3.0 μM Cyt-m, 3.0 μM PdR, 30 μM Pdx, ≈100 μM substrate and 3.7 mM NADH. Due to the low aqueous solubility of the substrates, separate vials were used for each time point to minimize the loss of substrate on the vials and pipettes during transfers; i.e., a complete reaction vial was sacrificed for each result. Reactions were stopped by the addition to each reaction vial of 0.5 g NaCl and 1 ml of organic solvent (hexane for tetralin based reactions—methylene chloride for GC-MS samples and non-tetralin GC samples). This addition was followed by vigorous mixing for 1 min. The emulsion which formed was broken down by centrifugation at ≈2200 $\times g_n$ for 10 min. The organic phase was then removed for analysis. Concentrations were determined from differences between the concentrations measured in reaction vials and those measured in the corresponding control vials. By coupling these concentrations with the sampling time, substrate disappearance and product generation rates were determined.

2.4.2.1. Cosolvent effect experiments. Determination of DMSO kinetic effects required reactions with the same enzyme–substrate mix with varied amounts of DMSO. This was achieved by making a master solution that consisted of 162.5 μM substrate, 6 μl/ml DMSO, 4.875 μM Cyt-m, 4.875 μM PdR, 48.75 μM Pdx and 80–99% vol/vol P-100. A volume of 2 ml of the master solution was added to each reaction vial. To this, P-100 and the desired amount of cosolvent totalling 0.75 ml were added to the vial. Several vials were chosen to serve as controls. The reactions and analysis then proceeded according to the method described in Section 2.4.2.

2.4.2.2. Stoichiometry experiments. These investigations were designed to determine the stoichiometric relationship between NADH utilization and substrate conversion. Two types of experimental measurements were needed to determine this relationship. NADH was measured spectrophotometrically, while substrates and products were measured using both GC and HPLC chromatographic methods. A volume of 2.75 ml of the master solution described above was pipetted into each vial. The methods from Section 2.4.2 were used with the following exceptions. All but two vials were used for determining substrate disappearance and product appearance rates. Reactions were started by the addition of 0.5 ml of 12 mM NADH. Lower NADH concentrations were necessary in order to ensure reliable NADH spectrophotometric data. Control vials (non-reacting samples representing initial conditions) were started by adding 0.5 ml of P-100.

NADH rates were determined using the two vials not used in the substrate and product rate experiment. Cuvettes with a 1.5 ml volume were prepared for spectrophotometric measurement of the solution NADH concentration by the addition of 950 μl of P-100. The spectrophotometer was blanked at 340 nm with one of the prepared cuvettes to which had been added a 50 μl sample from the control vial (2.75 ml master solution and 0.5 ml P-100). The reaction vial was started by the addition of 0.5 ml of 12 mM NADH. This vial was capped and then gently inverted to mix. Approximately every 100 s, 50 μl was withdrawn from the reaction vial. This 50 μl sample was added to a prepared cuvette, the reaction time was recorded, and the cuvette was gently inverted to mix the sample with the diluting P-100. The cuvette was inserted into the spectrophotometer, and the absorbance at 340 nm was recorded for ≈ 30 s at 1 s intervals. Changes in the NADH concentration which may have occurred during the lag between the time the 50 μl sample was diluted (recorded as the reaction time) and the spectrophotometric measurements began, were accounted for by extrapolating the 30 s sample NADH concentration record back to the dilution time. Using this method NADH concentrations were determined at ≈ 100 s intervals allowing the generation of NADH vs. time profiles. Comparison of the initial substrate and product rate data with this NADH profile were used to determine the stoichiometric relationship between NADH rate and hydroxylation rate.

2.4.2.3. Kinetic parameter experiments. Michaelis–Menten kinetic parameters were determined from initial rate data obtained from GC and HPLC measurements of substrate and product concentrations. Initial rate data was obtained on hydroxylation reactions that had conversions near 10% (4–15 min). Because of inaccuracies associated with the detection of tetralin, product generation was measured for these experiments. This necessitated the production of at least 5 μM (*R*)-1-tetralol to ensure that measurement errors were small compared to measured values. In reactions with low concentrations of tetralin this forced conversions up to 30%—well out of the range of initial rate data. The effect of this high conversion on the prediction of Michaelis–Menten parameters was reviewed. Theoretical analysis predicted no effect on ν_{max}. On the other hand, K_M for the tetralin–Cyt-m interaction was overestimated by 15%. This lower projected $K_{M,tetralin}$ falls within the experimental error and is more favorable than the one predicted strictly from the experimental data. The more conservative $K_{M,tetralin}$ prediction based strictly on the experimental data without theoretical adjustment was used.

Determination of Pdx dependent Michaelis–Menten parameters necessitated reactions with the same enzyme–substrate mix with varied amounts of Pdx. This was achieved by making a master solution that consisted of 162.5 μM substrate, 6 μl/ml DMSO, 4.875 μM Cyt-m, 4.875 μM PdR, 4.875 μM Pdx and 80–99% vol/vol P-100. A volume of 2 ml of this master solution was added to each reaction vial. To this, P-100 and the desired amount of Pdx totalling 0.75 ml were added to the vial. Several vials were chosen to serve as controls. The reactions and analysis then proceeded according to the method described in Section 2.4.2.

Determination of substrate dependent Michaelis–Menten parameters necessitated reactions with the same enzyme–cosolvent mix with varied amounts of substrate. For each substrate concentration tested both a non-reacting control and a reaction vial were needed. The control vial was used to determine the amount of substrate initially in the reaction due to possible substrate losses during transfers. This was achieved by making a master solution that consisted of no substrate, no DMSO, 3.55 μM Cyt-m, 3.55 μM PdR, 35.5 μM Pdx and 80–99% vol/vol P-100. To make these vials identical, 5.7 ml of the master solution was put into a 12 ml borosilicate test tube. A volume of 24.9 μl of substrate at the desired concentration dissolved in DMSO was added to the test tube.

This solution was mixed and then 2.75 ml was dispensed into each of two reaction vials. A volume of 0.5 ml of 24 mM NADH was added to the reacting vial and 0.5 ml of P-100 was added to the control. The reactions and analysis then proceeded according to the method described in Section 2.4.2.

3. Results and discussion

3.1. Hydroxylation of non-terpenes

The in vitro camphor 5-monooxygenase mediated biohydroxylations of a range of compounds was investigated using a standardized reaction procedure. The native substrate, camphor, and a structurally similar molecule, norcamphor, were used as reference compounds. The biohydroxylations of these reference compounds have been well studied [2,15–29] and illustrate the native behavior of the enzyme (see Fig. 1). The other substrates studied, naphthalene, tetralin and decalin, are cyclic hydrocarbons which are structurally different from camphor. They have hydroxylation products which are potential precursors for synthesizing biologically active substances [30–34]. The hydroxylation rates of these representative compounds were measured under conditions where reactions were only limited by Cyt-m and substrate concentrations.

Initial reaction rates based on substrate disappearance can be found in Table 2. These rates were normalized with respect to the Cyt-m active site concentrations. As would be expected, the fastest rates occurred with the native substrate camphor and the structurally similar norcamphor. The three naphthalene based substrates; naphthalene, decalin and tetralin, reacted three orders of magnitude more slowly than the terpene compounds. These slower rates suggest a poorer interaction between the hydrocarbon substrates and the enzyme active site within the Cyt-m subunit.

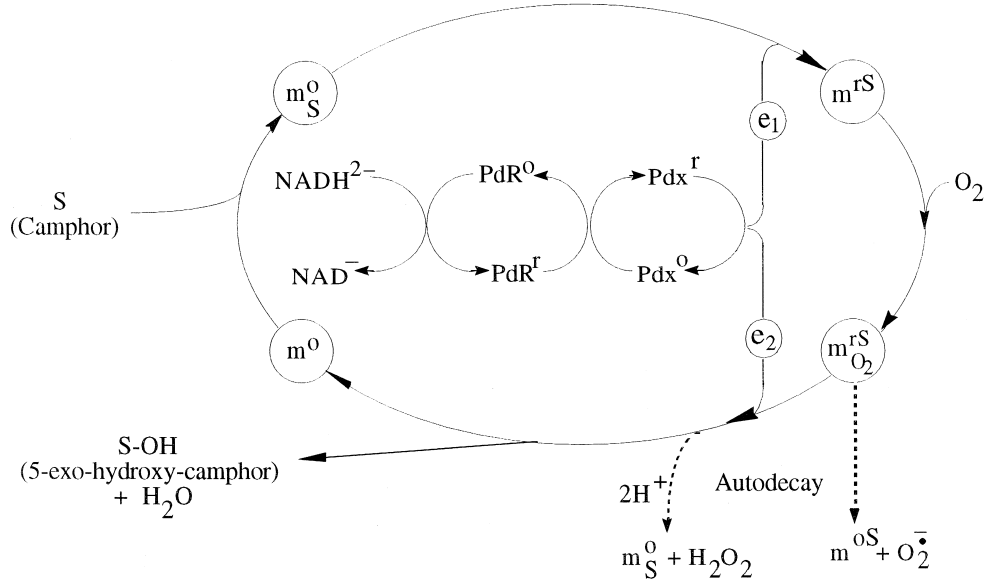

Fig. 1. Catalytic cycle for substrate (camphor) hydroxylation by the camphor (cytochrome *P*-450_{cam}) 5-monooxygenase system: (S) substrate, camphor; (m) cytochrome *P*-450_{cam} hydroxylase; ($NADH^{2-}$) nicotinamide adenine dinucleotide, reduced form; (NAD^-) nicotinamide adenine dinucleotide, oxidized form; (PdR) putidaredoxin reductase; (Pdx) putidaredoxin; (e_1) first electron transfer; (e_2) second electron transfer; (S–OH) hydroxylated substrate, 5-*exo*-hydroxycamphor; ($O_2^{-\cdot}$) superoxide complex; (superscript o) oxidized species; (superscript r) reduced species; (superscript S) substrate-bound species; (subscript O_2) oxygen-bound species. Adapted from Gunsalus et al. [35].

Table 2
Rates of camphor 5-monooxygenase mediated hydroxylation reactions

Substrate	Substrate utilization rate[a] (s^{-1})
camphor[b]	13 ± 4
norcamphor	0.203 ± 0.003
naphthalene	0.05 ± 0.01
tetralin	0.05 ± 0.02
decalin	0.06 ± 0.02

[a]The sample solutions (total volume 3.25 ml) contained substrate (≈ 90 μM), Cyt-m (3 μM), Pdx (30 μM), PdR (3 μM), DMSO (52 mM) and NADH (3.7 mM) in P-100. The reaction was carried out at 22°C. Rates are expressed in terms of active site turnovers (μmol substrate converted/μmol Cyt-m·s). The uncertainties in rates are equal to the standard error of the mean (a minimum of three measurements was performed to obtain each result).
[b]The camphor reaction is too quick to accurately measure initial rates by sampling techniques. There is a one to one correspondence between NADH and camphor utilization. Therefore, this rate was determined by spectrophotometrically following NADH usage of camphor reactions.

3.1.1. Cosolvent effects

The camphor 5-monooxygenase enzyme system has the ability to stereospecifically add a hydroxyl group to unactivated hydrocarbons creating specifically activated hydrocarbons which could potentially be used as precursors to valuable products. Unfortunately, this enzyme system is water soluble and unactivated hydrocarbons are not. Previously, we reported [9] that DMSO, methanol and 1,4-dioxane act as accelerators for the biohydroxylation of tetralin to (*R*)-1-tetralol. Without any discernible increase in tetralin solubility, the enzyme system with cosolvent had a rate up to five fold higher than the system without cosolvent. To optimize cosolvent concentration, hydroxylation rates of reaction (A1), tetralin to (*R*)-1-tetralol, were measured as a function of DMSO concentration as shown in Fig. 2. The addition of a small amount of DMSO dramatically increased the reaction rate, but continued increases in DMSO concentration led to decreasing rates. The DMSO volume percentage of 0.37%, used for the reactions in this paper, represents a compromise between having an accurately measurable amount of DMSO and maximizing reaction rate.

3.1.2. NADH and enzyme subunit concentration dependence

The camphor 5-monooxygenase enzyme system consists of the electron source NADH, and the three different enzyme subunits; Cyt-m, PdR and Pdx, all of which influence the rate of biohydroxylation. Cyt-m contains the active site of the camphor 5-monooxygenase enzyme system. All calculated rates were normalized by this concentration. By individually varying component concentrations, concentration sensitivity was evaluated for each component and expressed as Michaelis–Menten dissociation constants, K_M. Component concentrations less than twice K_M cause rates to decrease to less than two thirds of the maximum rate and exhibit near first order dependence on the concentration of the limiting component. With a concentration above nine times the value of K_M, the reaction will proceed at greater than 90% of the maximum rate with negligible changes in reaction rate for small changes in component concentration. Although it was developed to describe

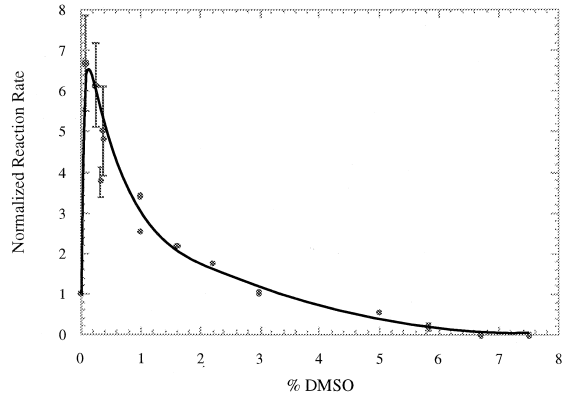

Fig. 2. Effect of DMSO on the camphor 5-monooxygenase hydroxylation of tetralin to (*R*)-1-tetralol. Reaction rates normalized by reaction rate without DMSO present. The sample solutions (total volume 3.25 ml) contained tetralin (≈ 100 μM), Cyt-m (3 μM), PdR (3 μM), Pdx (30 μM), DMSO at the indicated vol.% and NADH (3.7 mM) in buffer P-100. The reaction was carried out at 22°C. All rates of reaction are averages of product appearance and substrate disappearance within the first 8 min of reaction. The uncertainties in reaction rate are equal to the standard error of the data (at least three measurements were performed to obtain each result).

enzyme–substrate interactions, the Michaelis–Menten kinetic model:

$$\frac{\nu}{V_{\max}} = \frac{[S]}{[S] + K_M} \quad (1)$$

can also be used to quantitatively describe the interactions between the components of the camphor 5-monooxygenase enzyme system. Camphor 5-monooxygenase mediated biohydroxylation rates showed strong concentration dependence on all components, except PdR.

Roome published a Michaelis–Menten NADH dissociation constant of $K_{M,NADH} = 77 \pm 12$ μM [36]. This agreed well with screening experiments that showed camphor hydroxylation rates decreased markedly for NADH concentrations less than 200 μM. By working with NADH concentrations above 1 mM, NADH limitations were minimized.

Preliminary subunit screening reactions demonstrated that hydroxylation rates were least sensitive to the concentration of PdR. If the PdR concentration was equal to or greater than the Cyt-m concentration (≈ 3 μM), increases in PdR concentration had a negligible effect on hydroxylation rates. This seems to be contradicted by Roome and Peterson's measurement of PdR's Michaelis–Menten dissociation constant, $K_{M,PdR} = 139 \pm 25$ μM [36]. Roome and Peterson's $K_{M,PdR}$ was determined under conditions of limiting NADH (stoichiometric equivalence with PdR). When NADH was at concentrations from two to five times the PdR concentration, the Pdx–PdR interaction was much stronger [36]. In a production setting, NADH would be maintained at a level much higher than five times the PdR concentration. NADH is consumed by the reaction and would only be at low concentrations near the completion of a reaction cycle. Thus, for a commercial process, the effective $K_{M,PdR}$ will be smaller than that measured by Roome and Peterson, making PdR a non-limiting component. Accordingly, these experiments were conducted with concentration levels of NADH much higher than that of PdR.

The strong dependence of camphor 5-monooxygenase hydroxylation rates on Pdx concentration is attributed to electron transfer interactions as well as product release. Pdx cannot pass electrons to Cyt-m without substrate binding. Substrate binding raises the redox potential of Cyt-m to allow electron passage from Pdx to Cyt-m [35,37,38]. The rate limiting step of camphor biohydroxylation is the second electron transfer from Pdx to Cyt-m [35,38–43]. A 3 Pdx to 1 Cyt-m complex is the most effective coupling for this electron transport [35]. Pdx has also been shown to act as an effector in product release [32,38,39] with a concentration of 0.16 μM of oxidized Pdx being needed to produce half the maximal product yield [29]. Pdx's numerous interactions with Cyt-m signified an indirect interaction between substrate and Pdx which called for detailed investigation.

Simple kinetic studies were undertaken to examine substrate–Pdx interactions. Hydroxylation rates at varying Pdx concentrations were measured using camphor, (*R*)-1-tetralol, and two different concentrations of tetralin as substrate. Fig. 3 shows typical results from one of these experiments. Assuming Michaelis–Menten kinetics between Pdx and Cyt-m, nonlinear re-

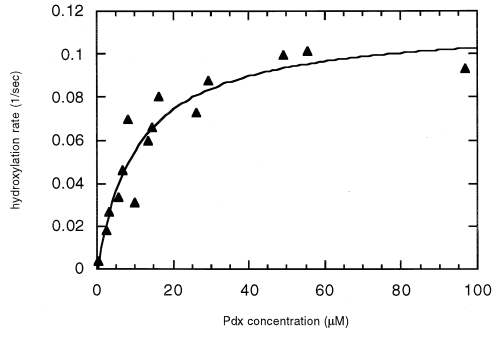

Fig. 3. Tetralin hydroxylation rate as a function of Pdx concentration used to calculate the Michaelis dissociation constant, $K_{M,Pdx}$, for the Pdx–Cyt-m complex. The sample solutions (total volume 3.25 ml) contained Pdx at the indicated concentrations, tetralin (330 μM), Cyt-m (3 μM), PdR (3 μM), DMSO (52 mM) and NADH (3.7 mM) in buffer P-100. The reactions were carried out at 22°C. All rates of reaction are averages of substrate disappearance within the first 8 min of reaction. The uncertainties in Pdx concentration are estimated to be $\approx 0.05 \times$[Pdx]; the uncertainties in hydroxylation rate are $\approx 0.1 \times$ rate.

gression of the Pdx concentration vs. hydroxylation rate data from each of the experiments was fit to the Michaelis–Menten equation:

$$\frac{\nu}{V'_{\max}} = \frac{[\mathrm{Pdx}]}{[\mathrm{Pdx}] + K_{\mathrm{M,Pdx}}}. \quad (2)$$

The calculated values of $V'_{\max}$ and $K_{\mathrm{M,Pdx}}$ are presented in Table 3. As expected, maximum hydroxylation rate, $V'_{\max}$, follows the same trends as the hydroxylation rates presented in Table 2. Less camphor-like substrates reacted slower and lower tetralin concentrations also exhibited slower reaction rates. The measured $K_{\mathrm{M,Pdx}}$s were essentially identical for all three substrates and at both tetralin concentrations. Thus, although different substrates caused different hydroxylation rates, these differences were not caused by substrate induced changes in the Pdx–Cyt-m interactions.

3.2. Biohydroxylation of tetralin to (R)-1-tetralol

The cell free camphor 5-monooxygenase mediated biohydroxylation of tetralin leads to ≈ 96% (*R*)-1-tetralol and 4% (*S*)-1-tetralol [9]. According to the Aldrich catalogue, (*R*)-1-tetralol is approximately 15,000 fold more valuable than tetralin. [2] This large increase in value illustrates the commercial potential of stereospecific hydrocarbon biohydroxylation reactions. It has also been shown that high concentrations of (*R*)-1-tetralol disappear from this system. Although isolation of this unknown product was not accomplished, HPLC retention times are consistent with what is expected for a dihydroxy derivative of tetralin. Such a product would be consistent with the operation of this enzyme system [9]. Thus, the overall tetralin biohydroxylation reaction is two reactions; reaction (A2) with tetralin as the substrate:

$$\mathrm{tetralin(aq)} + \mathrm{NADH^{-2}(aq)} + \mathrm{O_2(aq)} + \mathrm{H^+(aq)} \rightarrow (R)\text{-1-tetralol(aq)} + \mathrm{NAD^-(aq)} + \mathrm{H_2O(1)} \quad (A2)$$

and reaction (B) with (*R*)-1-tetralol as the substrate:

$$(R)\text{-1-tetralol(aq)} + \mathrm{NADH^{-2}(aq)} + \mathrm{O_2(aq)} + \mathrm{H^+(aq)} \rightarrow \mathrm{unknown(aq)} + \mathrm{NAD^-(aq)} + \mathrm{H_2O(1)}. \quad (B)$$

To understand this process a detailed stoichiometric and kinetic study of these reaction was conducted to develop a model of camphor 5-monooxygenase mediated biohydroxylation of tetralin.

3.2.1. Substrate–NADH stoichiometry

Camphor 5-monooxygenase mediated biohydroxylation involves the transfer of a pair of electrons from NADH, through the electron transport proteins; PdR and Pdx, into the active site found in Cyt-m. Here, the electrons activate the bound oxygen. The activated oxygen either reacts to yield the hydroxylated product and

Table 3
Effect of substrate on Pdx Michaelis–Menten parameters

Substrate	$K_{\mathrm{M,Pdx}}$	$V'_{\max}$
100 μM camphor	9.5 ± 2.2 μM	53 ± 3 s^{-1}
330 μM Tetralin	10.7 ± 2.2 μM	0.114 ± 0.009 s^{-1}
100 μM Tetralin	10.9 ± 2.2 μM	0.070 ± 0.004 s^{-1}
100 μM (*R*)-1-tetralol	11.4 ± 4.3 μM	0.034 ± 0.004 s^{-1}

(a) The sample solutions (total volume 3.25 ml) contained substrate at the indicated concentration, Cyt-m (3 μM), PdR (3 μM), DMSO (52 mM), NADH (3.7 mM) in buffer P-100, and varied amounts of Pdx. The reaction was carried out at 22°C. All rates of reaction are averages of substrate disappearance within the first 8 min of reaction. The uncertainties in substrate concentration are estimated to be ≈ 0.05 × [substrate]; the uncertainties in $K_{\mathrm{M,Pdx}}$ and $V_{\max}$ are equal to the standard error from the nonlinear regression of the data to fit Michaelis–Menten kinetic model (at least six measurements were performed to obtain each result).

[2] The 15,000 fold increase was based on calculations using the cost of the largest quantities available in the 1994/5 Aldrich catalog: tetralin 99% had a price of US$0.0123 g^{-1} while both (*R*)- and (*S*)-1-tetralol were priced at US$188.20 g^{-1}.

water or it is released without interacting with the substrate to form a hydroperoxide (see Fig. 1) [29]. The ability to successfully hydroxylate a substrate, instead of releasing a hydroperoxide, is dependent upon a number of factors; ease of hydrogen abstraction from the substrate, ease of hydroxyl addition to the oxidized substrate, and appropriate steric and hydrophobic interactions between the active site and the substrate to maintain the appropriate active site environment for reaction. The relationship between the initial rate of NADH utilization and the initial rate of substrate utilization is the substrate–NADH stoichiometry of this reaction. The stoichiometric ratio (molar rate of substrate utilization)/(molar rate of NADH oxidation) can be thought of as the efficiency of the reaction. When all of the available electrons are used to create products the stoichiometric ratio is one, but whenever unwanted hydroperoxides are generated the efficiency drops below one. Since NADH is consumed in this biohydroxylation reaction, NADH efficiency is an important factor in the overall cost of this biohydroxylation process.

Substrate–NADH stoichiometries were determined for the substrates camphor, tetralin and (*R*)-1-tetralol. These efficiencies along with published efficiencies for other substrates can be found in Table 4. The efficiencies were strongly influenced by substrate structure. Camphor and camphor like substrates were essentially perfect with nearly all of the available electrons being funnelled into the product. Hydrocarbons which were structurally different from camphor had efficiencies about an order of magnitude lower. The idea that Pdx–Cyt-m interactions are independent of substrate–Cyt-m interactions was reinforced by the discovery that concentration variations of the Pdx had a negligible effect on substrate–NADH efficiency. NADH efficiency for the substrate tetralin was $\approx 13 \pm 3\%$ and (*R*)-1-tetralol degradation was even less efficient at $\approx 7.8 \pm 0.7\%$. These new results agree well with the results previously published for non camphor-like substrates which have NADH efficiencies of approximately 10%.

Table 4
Effect of substrate on substrate–NADH stoichiometry

Substrate	Efficiency (100%·substrate utilized/NADH utilized)	References
camphor[a]	$100 \pm 4\%$	This work
thiocamphor	98%	[44]
tetralin[a]	$15 \pm 3\%$	This work
tetralin (5 μM Pdx)[b]	$12 \pm 4\%$	This work
norcamphor	12%	[15,28]
camphane	8%	[44]
(*R*)-1-tetralol[a]	$7.8 \pm 0.7\%$	This work
ethylbenzene	5%	[4]
styrene	2.2%	[3]
cis-β-methylstyrene	1.0%	[3]

[a]The sample solutions (total volume 3.25 ml) contained substrate (≈ 100 μM), Cyt-m (3 μM), Pdx (30 μM except where noted), PdR (3 μM), DMSO (52 mM) and NADH (1.85 mM) in P-100. The reaction was carried out at 22°C. Efficiency is expressed in terms of percentage (100% × μmol substrate converted/μmol NADH used). The uncertainties in efficiencies are equal to the standard error of the mean (a minimum of three measurements was performed to obtain each result).
[b]The conditions are identical to those described in tablenote a except that the concentration of Pdx was 5 μM.

3.2.2. Substrate Michaelis–Menten kinetics

Camphor 5-monooxygenase enzyme system Michaelis–Menten kinetic parameters were individually determined for the substrates tetralin and (*R*)-1-tetralol. Secondary reactions and product inhibition effects were avoided by using data from initial rate experiments. These were performed at varying concentrations of tetralin and (*R*)-1-tetralol. NADH and PdR were present in excess concentrations, and the same Pdx concentration was used for all reactions. Assuming simple Michaelis–Menten kinetics, Eq. (1) was used to obtain substrate dependent K_M and V'_{max} from nonlinear regressions of turnover rate vs. substrate concentration plots. Tetralin's Michaelis constant, $K_M = 66 \pm 26$ μM, suggests that it binds much more tightly to the active site than does (*R*)-1-tetralol with a Michaelis constant of $K_M = 2800 \pm 1300$ μM. The limiting rates exhibit just the opposite behavior. Strongly binding tetralin reacts with a limiting rate of $V'_{max} = 0.05 \pm 0.01\ s^{-1}$. This is

almost an order of magnitude slower than weakly bound (*R*)-1-tetralol's rate of $V'_{max} = 0.4 \pm 0.1\ s^{-1}$.

3.2.3. Kinetic model

A model of the camphor 5-monooxygenase enzyme system was constructed to predict the substrate and product profiles as a function of time for the conversion of tetralin. As previously stated, the biohydroxylation of tetralin is actually two simultaneous reactions, reaction (A2) and reaction (B). Although these are the proper chemical reactions, they are not appropriate for modelling this biohydroxylation process. The model focuses on the limiting species in each of the 'streams' leading to the active site within the cytochrome *P*-450_{cam} hydroxylase subunit.

The substrate stream consists of the substrates and cosolvents: tetralin, (*R*)-1-tetralol, oxygen and DMSO. DMSO concentration can have a strong influence on the reaction rate (Fig. 2) but, for the purposes of this model DMSO concentration was considered constant. Biohydroxylation reactions were performed to test the effect of oxygen concentration. It was found that air saturated systems and oxygen saturated systems (containing five times more oxygen) exhibited no significant differences in reaction rate nor in product formation. Thus, the substrates, tetralin and (*R*)-1-tetralol, were the only species from the first stream considered to be of kinetic import. The power stream consists of the species which supply and transfer the reducing power to the active site. In the preceding sections, we have demonstrated that PdR and NADH can be made available in non-limiting concentrations. Pdx concentration had a significant influence on reaction rate (see Fig. 3). The important species identified by this stream analysis for inclusion in the tetralin biohydroxylation model were: Cyt-m (the active site), tetralin (first stream), (*R*)-1-tetralol (first stream) and Pdx (second stream).

The substrates, tetralin and (*R*)-1-tetralol, compete for the same active site in the Cyt-m subunit. Thus, it was important to consider these reactions simultaneously. Focusing on the kinetically important species as determined by the stream analysis, reaction (A2), the conversion of tetralin to (R)-1-tetralol was rewritten as:

$$\text{Cyt-m} + \text{tetralin} \underset{k_{-1}}{\overset{k_1}{\leftrightarrow}} \text{Cyt-m–tetralin} \xrightarrow{k_2} (R)\text{-1-tetralol} + \text{Cyt-m} \quad \text{(C)}$$

and reaction (B), the conversion of (*R*)-1-tetralol to 'unknown', was rewritten as:

$$\text{Cyt-m} + (R)\text{-1-tetralol} \underset{k_{-3}}{\overset{k_3}{\leftrightarrow}} \text{Cyt-m–}(R)\text{-1-tetralol} \xrightarrow{k_4} \text{unknown} + \text{Cyt-m}. \quad \text{(D)}$$

Using standard Michaelis–Menten analysis techniques, a pair of coupled velocity equations were developed for these two reactions. The resulting equations were for the tetralin hydroxylation reaction (C):

$$\nu_1 = \frac{V'_{1\text{-max}}[\text{tetralin}]}{[\text{tetralin}] + K_{M1}\left(1 + \dfrac{[(R)\text{-1-tetralol}]}{K_{M2}}\right)} \quad (3)$$

and for the (*R*)-1-tetralol to 'unknown' reaction (D):

$$\nu_2 = \frac{V'_{2\text{-max}}[(R)\text{-1-tetralol}]}{[(R)\text{-1-tetralol}] + K_{M2}\left(1 + \dfrac{[\text{tetralin}]}{K_{M1}}\right)} \quad (4)$$

where ν_1 is the predicted rate of (*R*)-1-tetralol production, $V'_{1\text{-max}}$ is the maximum possible value of ν_1 (for a given Pdx concentration), ν_2 is the predicted rate of (*R*)-1-tetralol disappearance, $V'_{2\text{-max}}$ is the maximum possible value of ν_2 (for a given Pdx concentration), K_{M1} is the Michaelis constant associated with the dissociation of the tetralin–Cyt-m complex, and K_{M2} is the Michaelis constant associated with the dissociation of the (*R*)-1-tetralol–Cyt-m complex.

Eqs. (3) and (4) take into account all of the substrate competition at the active site, but do not account for the effects of Pdx concentration.

Cytochrome $P\text{-}450_{cam}$ hydroxylase (Cyt-m) interactions with Pdx are not influenced by substrate–Cyt-m interactions. The consistent K_M values found in Table 3 illustrate that, although Pdx–Cyt-m binding is dependent on binding of a substrate, the identity of the substrate does not influence the binding. Thus, Pdx was treated as an independent entity that only effected the V'_{max} of the reactions. Fig. 3 shows the effect of Pdx concentration on biohydroxylation and this effect is expressed in Eq. (2). Multiplying the right hand side of both Eqs. (3) and (4) by the right hand side of Eq. (2), two equations were developed that not only reflect substrate active site interactions, but also account for the interaction with Pdx. For the conversion of tetralin to (*R*)-1-tetralol the velocity equation becomes:

$$\nu_1 = \left(\frac{V_{1\text{-max}}[\text{tetralin}]}{[\text{tetralin}] + K_{M1}\left(1 + \frac{[R\text{-1-tetralol}]}{K_{M2}}\right)} \right) \times \left(\frac{[\text{Pdx}]}{[\text{Pdx}] + K_{M,\text{Pdx}}} \right) \quad (5)$$

and the (*R*)-1-tetralol to 'unknown' velocity equation becomes:

$$\nu_2 = \left(\frac{V_{2\text{-max}}[R\text{-1-tetralol}]}{[R\text{-1-tetralol}] + K_{M2}\left(1 + \frac{[\text{tetralin}]}{K_{M1}}\right)} \right) \times \left(\frac{[\text{Pdx}]}{(\text{Pdx}) + K_{M,\text{Pdx}}} \right) \quad (6)$$

where [Pdx] is the molar concentration of Pdx, $K_{M,Pdx}$ is the Michaelis constant associated with the dissociation of the Pdx–Cyt-m complex, and the rest of the variables are as described for Eqs. (3) and (4) except $V_{1\text{-max}}$ and $V_{2\text{-max}}$ which are maximum velocities at infinite concentrations of both substrate and Pdx. With the exception of changes in cosolvent concentration, Eqs. (5) and (6) account for all of the critical interactions in the biohydroxylation of tetralin.

Table 5
Michaelis–Menten kinetic model parameters

Limiting component	K_M (μM^{-1})	V^a_{Max} (s^{-1})
Pdx	$K_{M,Pdx} = 10.6 \pm 2$	–
tetralin	$K_{M1} = 66 \pm 27$	$V_{1-max} = 0.107 \pm 0.035$
(*R*)-1-tetralol	$K_{M2} = 2{,}800 \pm 1300$	$V_{2-max} = 0.83 \pm 0.22$

[a] Extrapolated to infinite Pdx concentration.

The Michaelis–Menten kinetic parameters determined from initial reaction rates used for this model can be seen in Table 5. The Michaelis binding constants measured in Section 3.2.2 were used for K_{M1} (tetralin) and for K_{M2} ((*R*)-1-tetralol). The Pdx Michaelis binding constant, $K_{M,Pdx}$, used was an average of the values found in Table 3. All of the previously presented V'_{1-max} and V'_{2-max} rates reflect either infinite Pdx concentration (Table 3) or infinite substrate concentration. Using these V'_{max} values, experimental conditions and Eqs. (5) and (6), V_{max} values were extrapolated for infinite concentrations of both Pdx and substrate.

Eqs. (5) and (6) were used along with the results from the stoichiometric experiments to develop equations to predict concentration changes to substrate (Eq. (7)), cofactor (Eq. (8)) and product (Eqs. (9) and (10)).

$$\frac{d}{dt}[\text{tetralin}] = -\frac{\nu_1}{0.96} \quad (7)$$

$$\frac{d}{dt}[\text{NADH}] = \frac{\nu_1}{0.13} + \frac{\nu_2}{0.078} \quad (8)$$

$$\frac{d}{dt}[(R)\text{-1-tetralol}] = \nu_1 - \nu_2 \quad (9)$$

$$\frac{d}{dt}[(S)\text{-1-tetralol}] = \frac{0.04}{0.96}\nu_1 - \nu_2^* \quad (10)$$

where ν_2^* is ν_2 as a function of [(*S*)-1-tetralol] [3], thus all [(*R*)-1-tetralol] in Eq. (6) are replaced by [(*S*)-1-tetralol]. Using an initial condition of 80 μM tetralin and 1.6 mM NADH,

[3] In an attempt to identify the 'unknown' product, the degradation of (*S*)-1-tetralol was performed. It was found that (*S*)-1-tetralol degradation followed the same kinetics as (*R*)-1-tetralol.

simultaneous Newton iterations were performed on Eqs. (5)–(7), (9) and (10). The resulting substrate and product profiles were plotted along with data from a pair of experiments and can be seen in Fig. 4. NADH profiles seen in Fig. 5 were generated for Eq. (8) using the same method. There is strong agreement between the experimental data points and the model.

For the first 800 s, the model estimate and experimental data points almost coincide, but after this initial phase, the model begins to overestimate the reaction rate. At about 800 s, the NADH concentration drops below 1 mM, out of the range for which the model was developed (see Fig. 5). The reaction rates are limited by NADH availability. These limiting conditions would not occur during a production run, but were necessary to confirm NADH tracking by the model. At higher NADH concentrations the spectrophotometric signal became too strong and high dilutions were needed to obtain readings. Unfortunately, the necessary dilutions were so high (greater than 25 fold) that the noise they introduced made measurement of concentration impossible. By keeping the NADH concentration lower, reliable spectrophotometric data were obtained. As seen in the figure, this forced some experimental data into a region not applicable to the model.

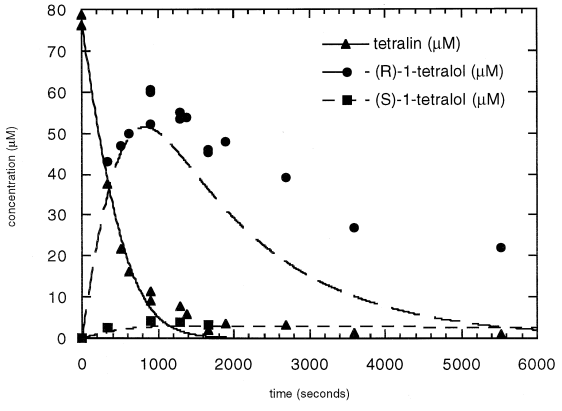

Fig. 4. Time course plot of substrate and product concentration during the conversion of tetralin by the camphor 5-monooxygenase enzyme system. The sample solutions (total volume 3.25 ml) contained tetralin (80 μM), Cyt-m (3 μM), PdR (3 μM), Pdx (30 μM), DMSO (52 mM) and NADH (1.6 mM) in buffer P-100. The reactions were carried out at 22°C. The symbols are: (▲) tetralin, (●) (*R*)-1-tetralol and (■) (*S*)-1-tetralol. The lines are predictions based on the Michaelis–Menten kinetic model of the system Eqs. (5)–(10). The uncertainties in concentrations are estimated to be approximately 5% of the measured value down to a minimum error of approximately 3 μM. This figure should be looked at in conjunction with the NADH profile which can be seen in Fig. 5.

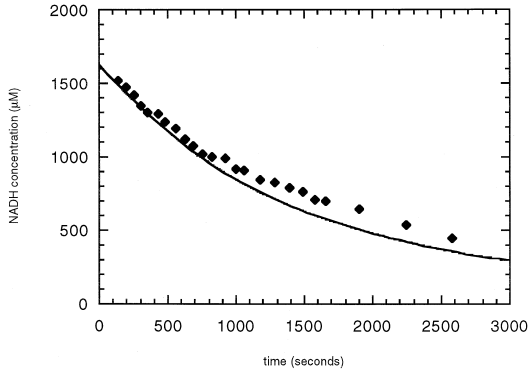

Fig. 5. Time course plot of NADH during the conversion of tetralin by the camphor 5-monooxygenase enzyme system. The sample solutions (total volume 3.25 ml) contained tetralin (80 μM), Cyt-m (3 μM), PdR (3 μM), Pdx (30 μM), DMSO (52 mM) and NADH (1.6 mM) in buffer P-100. The reactions were carried out at 22°C. The NADH concentrations were measured spectrophotometrically. The symbol (♦) represents NADH. The line represents the prediction based on the Michaelis–Menten kinetic model of the system, Eq. (8). This figure should be looked at in conjunction with the substrate and product profiles which are seen in Fig. 4.

An interesting and potential valuable behavior is seen in the reaction after 1000 s. At this point tetralin is exhausted and (*R*)-1-tetralol begins to be consumed. This makes sense. Although (*R*)-1-tetralol can potentially degrade eight times faster than it can be formed from tetralin, the much weaker binding of (*R*)-1-tetralol with the active site allows tetralin to out compete (*R*)-1-tetralol for the active site. From the model, we can predict that $\nu_1/\nu_2 = 5.46$ [tetralin]/[(*R*)-1-tetralol]. Thus, tetralin will react faster than (*R*)-1-tetralol until the concentration of (*R*)-1-tetralol is more than five times that of tetralin. This behavior is likely to be repeated with most hydrocarbon substrate-hydroxylated product pairs reacting with this system. The product will be chemically easier to hydroxylate because of its hydroxyl group, but that same hydroxyl group will decrease its affinity for the active site. Thus, it will be easy to

limit the amount of secondary reaction, by simply removing as much product as possible during the course of the reaction or alternatively by starting with excessive amounts of substrate.

In summary, the above data and model show that the camphor 5-monooxygenase enzyme system can be used to produce valuable chiral products from unactivated cycloarene substrates. A simple Michaelis–Menten kinetic model based on initial rate data is sufficient to predict substrate utilization, and product generation as well as NADH and cofactor usage.

Acknowledgements

We thank Dr. Jesse Edwards (National Institute of Standards and Technology) for performing the high-resolution two-dimensional gel electrophoresis separations, Mr. Edward Ruth (Department of Civil and Environmental Engineering, UCLA) for performing the gas chromatography electron-impact mass spectroscopy and Mr. Martin Mayhew for supplying much of the purified protein used in this work. Funding support from the National Science Foundation (Grant CATS 9313009) and Du Pont is gratefully acknowledged.

References

[1] R.E. White, M.B. McCarthy, K.D. Egeberg, S.G. Sligar, Arch. Biochem. Biophys. 228 (1984) 493.
[2] P.V. Gould, M.H. Gelb, S.G. Sligar, J. Biol. Chem. 256 (1981) 6686.
[3] J.A. Fruetel, J.R. Collins, D.L. Camper, G.H. Loew, P.R. Ortiz de Montellano, J. Am. Chem. Soc. 114 (1992) 6987.
[4] P.J. Loida, S.G. Sligar, Protein Eng. 6 (1993) 207.
[5] C.E. Castro, R.S. Wade, N.O. Belser, Biochemistry 24 (1985) 204.
[6] S. Li, L.P. Wackett, Biochemistry 32 (1993) 9355.
[7] G.S. Koe, V.L. Vilker, Biotech. Prog. 9 (1993) 608.
[8] T.L. Poulos, B.C. Finzel, A.J. Howard, Biochemistry 195 (1987) 687.
[9] D.A. Grayson, Y.B. Tewari, M.P. Mayhew, V.L. Vilker, R.N. Goldberg, Arch. Biochem. Biophys. 332 (1996) 239.
[10] J.A. Peterson, E.J. McKenna, R.W. Estabrook, M.J. Coon, Arch. Biochem. Biophys. (1969) 245.
[11] A.H. Phillips, R.G. Langdon, J. Biol. Chem. 237 (1962) 2652.
[12] J.J. Edwards, D.J. Reader, D.H. Atha, Appl. Theoret. Electroph. 1 (1990) 207.
[13] S.R. Heller, G.W.A. Milne, EPA-NIH Mass Spectral Data Base, US Department of Commerce, WA, 1983.
[14] I.C. Gunsalus, G.C. Wagner, Methods Enzymol. 52C (1978) 166.
[15] W.M. Atkins, S.G. Sligar, J. Am. Chem. Soc. 109 (1987) 3754.
[16] H.E. Conrad, R. DuBus, M.J. Namtvedt, I.C. Gunsalus, J. Biol. Chem. 240 (1965) 495.
[17] F.S. Sariaslani, Adv. Appl. Microbiol. 36 (1991) 133.
[18] M.H. Gelb, D.C. Heimbrook, P. Malkonen, S.G. Sligar, Biochemistry 21 (1982) 370.
[19] B.W. Griffin, J.A. Peterson, Biochemistry 11 (1972) 4740.
[20] I.C. Gunsalus, S.G. Sligar, Biochemie 58 (1976) 143.
[21] I.C. Gunsalus (Ed.), National Research Council, Degradation of Synthetic Organic Molecules in the Biosphere, San Francisco, CA, 12–13 June 1971, p. 137.
[22] J. Hedegaard, I.C. Gunsalus, J. Biol. Chem. 240 (1965) 4038.
[23] R. Lange, J. Pierre, P. Debey, Eur. J. Biochem. 107 (1980) 441.
[24] R.L. Tsai, I.C. Gunsalus, K. Dus, Biochem. Biophys. Res. Commun. 45 (1971) 1300.
[25] J.A. Peterson, Arch. Biochem. Biophys. 144 (1971) 678.
[26] J.R. Collins, G.H. Loew, J. Biol. Chem. 263 (1988) 3164.
[27] R. Raag, T.L. Poulos, Biochemistry 30 (1991) 2674.
[28] W.M. Atkins, S.G. Sligar, J. Am. Chem. Soc. 111 (1989) 2715.
[29] J.D. Lipscomb, S.G. Sligar, M.J. Namtvedt, I.C. Gunsalus, J. Biol. Chem. 251 (1976) 1116.
[30] S.O. Ukerun, Liebigs Ann. Chem. 9 (1989) 929.
[31] W.M. Welch, C.A. Harbert, R. Sarges, W.P. Stratten, A. Weissman, J. Med. Chem. 20 (1977) 699.
[32] K.T. Wan, M.E. Davis, J. Catal. 148 (1994) 1.
[33] A.P. Monte, D. Marona-Lewicka, N.V. Cozzi, D.E. Nichols, J. Med. Chem. 36 (1993) 3700.
[34] K. Christova, D. Dantschev, Arch. Pharm. (Weinheim) 311 (1978) 948.
[35] I.C. Gunsalus, J.R. Meeks, J.D. Lipscomb, Ann. New York Acad. Sci. (1973–74) p. 107.
[36] P.W. Roome, J.A. Peterson, Arch. Biochem. Biophys. 266 (1988) 41.
[37] S.G. Sligar, I.C. Gunsalus, Proc. Natl. Acad. Sci. U.S.A. 73 (1976) 1078.
[38] S.G. Sligar, R.I. Murray, in: P.R. Ortiz de Montellano (Ed.), Cytochrome *P*-450$_{cam}$ and Other Bacterial *P*-450 Enzymes, New York, 1986, p. 429.
[39] C.B. Brewer, J.A. Peterson, J. Biol. Chem. 263 (1988) 791.
[40] P.S. Stayton, S.G. Sligar, Biochemistry 29 (1990) 7381.
[41] M.D. Davies, L. Qin, J.L. Beck, K.S. Suslick, H. Koga, T. Horiuchi, S.G. Sligar, J. Am. Chem. Soc. 112 (1990) 7396.
[42] C.A. Tyson, J.D. Lipscomb, I.C. Gunsalus, J. Biol. Chem. 247 (1972) 5777.
[43] H.-G. Muller, W.-H. Schunck, P. Riege, H. Honeck, in: K. Ruckpaul, H. Rein (Eds.), Cytochrome *P*-450 of Microorganisms, Berlin, 1984, p. 337.
[44] W.M. Atkins, S.G. Sligar, J. Biol. Chem. 263 (1988) 18842.